Int. J. Electrochem. Sci., 7 **(2012)** 10215 - 10232

International Journal of
ELECTROCHEMICAL
SCIENCE
www.electrochemsci.org

The Adsorption and Corrosion Inhibition of 2-[Bis-(3,5-dimethyl-pyrazol-1-ylmethyl)-amino]-pentanedioic Acid on Carbon Steel Corrosion in 1.0 m HCl

A. Zarrouk[1,*], *H. Zarrok*[2], *R. Salghi*[3], *N. Bouroumane*[1], *B. Hammouti*[1], *S. S. Al-Deyab*[4], *R. Touzani*[1,5]

[1] LCAE-URAC18, Faculté des Sciences, Université Mohammed 1er, Oujda, Morocco.
[2] Laboratoire des procèdes de séparation, Faculté des Sciences, Université Ibn Tofail, Kénitra, Morocco.
[3] Equipe de Génie de l'Environnement et Biotechnologie, ENSA, Université Ibn Zohr, BP1136 Agadir, Morocco.
[4] Petrochemical Research Chair, Chemistry Department, College of Science, King Saud University, P.O. Box 2455, Riyadh 11451, Saudi Arabia.
[5] LCAE-URAC18, Faculté Polydisciplinaire, Université Mohammed Premier, Nador, Morocco.
[*]E-mail: azarrouk@gmail.com

Received: 11 August 2012 / *Accepted:* 6 September 2012 / *Published:* 1 October 2012

In this study, we investigated the inhibition of the corrosion of carbon steel (CS) in acidic solution by 2-[Bis-(3,5-dimethyl-pyrazol-1-ylmethyl)-amino]-pentanedioic acid (Bip1) was studied against carbon steel corrosion, in acidic environment using weight loss and electrochemical measurements. The inhibition efficiency increased with increasing inhibitor's concentration, but decreased with the increase in temperature. Bip1 acted as a highly efficient mixed type inhibitor. Adsorption of used inhibitor led to a reduction in the double layer capacitance and an increase in the charge transfer resistance. The high inhibition efficiency was attributed to the blocking of active sites by adsorption of inhibitor molecules on the steel surface. The adsorption of Bip1 on the carbon steel surface obeyed Langmuir adsorption isotherm. The inhibition mechanism was further corroborated by the values of activation parameters obtained from the experimental data.

Keywords: Pyrazole, Steel, Corrosion inhibition, Polarization curves, EIS.

1. INTRODUCTION

Acid solutions are widely used in industry, such as acid pickling, industrial acid cleaning, acid descaling and oil-well cleaning [1]. As the most effective and economic method [2,3], inhibitors are applied in these processes to control the metal dissolution. Most of the well known acid inhibitors are

organic compounds containing nitrogen, sulphur and oxygen atoms. The efficiency of these compounds mainly depends on their abilities to be adsorbed on the metal surface with the polar groups acting as the reactive centers.

In recent years, there is a considerable amount of effort devoted to develop novel and efficient corrosion inhibitors, and some compounds containing sulphur and/or nitrogen have been found to be effective corrosion inhibitors [4–20]. The organic inhibitors function through adsorption on metal surface blocking the active sites by displacing water molecules and forming a compact barrier film to decrease the corrosion rate [21]. The adsorption of inhibitors on metal / solution interface is influenced by: (*i*) nature and surface charge of metal; (*ii*) type of aggressive electrolyte; and (*iii*) chemical structure of inhibitors [22].

The objectives of this work were to study the inhibition performance of novel synthesized nonionic surfactants on carbon steel in 1.0 M HCl solution using weight loss and electrochemical techniques. Thermodynamic parameters of inhibitor adsorption on the metal surface and metal dissolution were also studied. The chemical structure of the studied bipyrazole derivative is given in Fig 1.

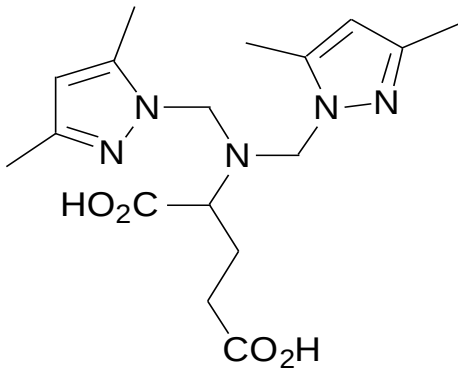

Figure 1. The chemical structure of the studied bipyrazolic compound.

2. EXPERIMENTAL METHODS

2.1. Materials

The steel used in this study is a carbon steel (Euronorm: C35E carbon steel and US specification: SAE 1035) with a chemical composition (in wt%) of 0.370 % C, 0.230 % Si, 0.680 % Mn, 0.016 % S, 0.077 % Cr, 0.011 % Ti, 0.059 % Ni, 0.009 % Co, 0.160 % Cu and the remainder iron (Fe). The carbon steel samples were pre-treated prior to the experiments by grinding with emery paper SiC (120, 600 and 1200); rinsed with distilled water, degreased in acetone in an ultrasonic bath immersion for 5 min, washed again with bidistilled water and then dried at room temperature before use. The acid solutions (1.0 M HCl) were prepared by dilution of an analytical reagent grade 37 % HCl with double-distilled water. The concentration range of Bip1 employed was 10^{-6} M to 10^{-3} M.

2.2. Synthesis

In the studied, the tridentate compound presented in Figure 1, which is tested as corrosion inhibitor was synthesized according to our used and known experimental methods [23-35]. The compound has been prepared by condensation of one equivalent of the (3,5-Dimethyl-pyrazol-1-yl)-methanol and one equivalent of the 2-Amino-pentanedioic acid in acetonitril as solvent, by stirring during four days at room temperature. The product has been purified and characterized by ^{1}H NMR, ^{13}C NMR spectroscopy and mass spectroscopy analysis.

2.3. Measurements

2.3.1. Weight loss measurements

The steel sheets of 1.6 × 1.6 × 0.07 cm dimensions were abraded with different grades of emery papers, washed with distilled water, degreased with acetone, dried and kept in a desiccator. After weighing accurately by a digital balance with high sensitivity the specimens were immersed in solution containing 1.0 M HCl solution with and without various concentrations of the investigated inhibitor. After 6 h exposure, the specimens were taken out rinsed thoroughly with bi-distilled water, dried and weighted accurately again. Three parallel experiments were performed for each test. The average weight loss, ΔW (mg) was calculated using the following equation [36]:

$$\Delta W = W1 - W2 \quad (1)$$

where W1 and W2 are the average weight of specimens before and after exposure, respectively.

2.3.2. Electrochemical measurements

The electrochemical measurements were carried out using Volta lab (Tacussel- Radiometer PGZ 100) potentiostate and controlled by Tacussel corrosion analysis software model (Voltamaster 4) at under static condition. The corrosion cell used had three electrodes. The reference electrode was a saturated calomel electrode (SCE). A platinum electrode was used as auxiliary electrode of surface area of 1 cm^2. The working electrode was carbon steel. All potentials given in this study were referred to this reference electrode. The working electrode was immersed in test solution for 30 minutes to a establish steady state open circuit potential (E_{ocp}). After measuring the E_{ocp}, the electrochemical measurements were performed. All electrochemical tests have been performed in aerated solutions at 308 K. The polarization curves were obtained in the potential range from -700 to -250 mV(SCE) with 1 mV s^{-1} scan rate. The EIS experiments were conducted in the frequency range with high limit of 100 kHz and different low limit 0.1 Hz at open circuit potential, with 10 points per decade, at the rest potential, after 30 min of acid immersion, by applying 10 mV ac voltage peak-to-peak. Nyquist plots were made from these experiments. The best semicircle can be fit through the data points in the Nyquist plot using a non-linear least square fit so as to give the intersections with the *x*-axis.

3. RESULTS AND DISCUSSION

3.1. Gravimetric study

3.1.1. Effect of concentration

The corrosion rate (A) of steel specimens after 6 h exposure to 1.0 M HCl solution with and without the addition of various concentrations of the investigated inhibitor was calculated and the obtained data are listed in Table 1. The variation of A with inhibitor concentration is shown in Fig. 2. The corrosion rate, A (mg cm^{-2} h^{-1}), surface coverage (θ) and inhibition efficiency η_w of each concentration were calculated using the following equations [37]:

$$A = \frac{\Delta W}{St} \quad (2)$$

$$\theta = \frac{A_{uninh} - A_{inh}}{A_{uninh}} \quad (3)$$

$$\eta_w = \left(\frac{A_{uninh} - A_{inh}}{A_{uninh}} \right) \times 100 \quad (4)$$

where ΔW is the average weight loss (mg), S is the surface area of specimens (cm^2), and t is the immersion time (h), A_{uninh} and A_{inh} are corrosion rates in the absence and presence of inhibitor, respectively.

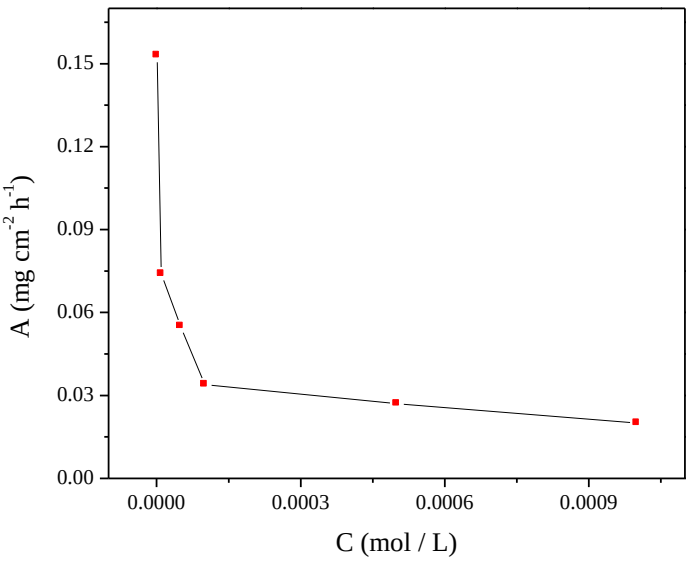

Figure 2. Relationship between the corrosion rate and inhibitor concentration for steel after 6 h immersion in 1.0 M HCl at 308 K.

Table 1. Corrosion parameters obtained from weight loss measurements for carbon steel in 1.0 M HCl containing various concentration of inhibitor at 308 K.

Inhibitor	Conc (M)	*A* (mg/cm^2 h)	η_w (%)	θ
Blank	1	1.070	-----	-----
Bip1	1×10^{-3}	0.020	98.1	0.981
	5×10^{-4}	0.027	97.5	0.975
	1×10^{-4}	0.034	96.8	0.968
	5×10^{-5}	0.055	94.9	0.949
	1×10^{-5}	0.074	93.1	0.931
	1×10^{-6}	0.153	85.7	0.857

It is clear that η_w increased with increasing inhibitor concentration, while corrosion rate decreased. This could be due to the inhibitor molecules act by adsorption on the metal surface [38]. The variation of η_w and inhibitor concentration in 1.0 M HCl solution at 308 K is shown in Fig. 3. When the concentration of inhibitor is less than 10^{-3}M, the η_w increased with an increase in concentration, while a further increase causes no appreciable change in performance. The maximum η_w value of (10^{-3}M) of this inhibitor is 98.1%. It was shown that the protective properties of such compounds depend upon their ability to reductive corrosion rate and are enhanced at higher electron densities around the heterocyclic and nitrogen atoms specially. The organic compounds containing electron negative function groups and π electrons conjugated are usually good inhibitors. Authors reported that the heteroatoms are the adsorption centers for interactions with the metal surface that permitted to reinforce this interaction [39, 40].

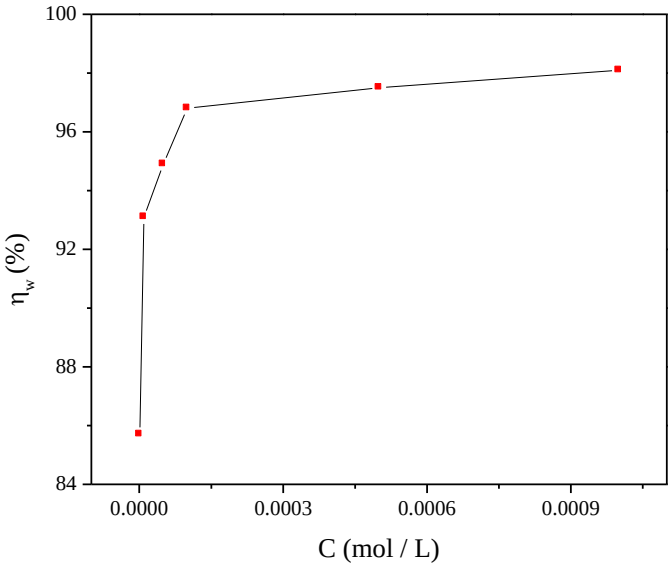

Figure 3. Relationship between the inhibition efficiency and inhibitor concentration for steel after 6 h immersion in 1.0 M HCl at 308 K.

In the present tests, this inhibitor possesses two rings in their structure with two nitrogen atoms forming a part of the ring. These types of molecule are stable corrosion inhibitors in acid due to the nitrogen atoms, active center of adsorption. The high inhibition efficiency for 2-[Bis-(3,5-dimethyl-pyrazol-1-ylmethyl)-amino]-pentanedioic acid (Bip1), was attributed to the presence of electron donor groups (-CH_3) in their structure. The adsorption the compounds organic on the metal surface can occur either d-orbital of iron surface atoms or an interaction of organic nitrogen compounds with already adsorbed directly on the basis of donor–acceptor interactions between the π-electrons of the ring and the vacant groups as proposed in literature [41,42].

3.1.2. Effect of temperature

Temperature is an important parameter in studies on metal dissolution [43]. The corrosion rate in acid solutions, for example, increases exponentially with temperature increase because the hydrogen evolution overpotential decreases [44]. To assess the effect of temperature on corrosion and corrosion inhibitive process, weight loss experiments were performed in the temperature range 308-343K in uninhibited acid (1.0 M HCl) and in inhibited solutions containing different concentrations of Bip1. The corresponding data are shown in Table 2. The relationship between the corrosion rate (A) of steel in acidic media and temperature (T*)* is often expressed by the Arrhenius equation [45]:

$$LnA = Lnk - \frac{E_a}{RT} \qquad (5)$$

where A is the corrosion rate, E_a is the apparent activation energy, R is the molar gas constant (8.314 J K^{-1} mol^{-1}), T is the absolute temperature, and k is the frequency factor. The fractional surface coverage θ can be easily determined from weight loss measurements by the ratio η_w% / 100 if one assumes that the values of η_w% do no differ substantially from θ.

Table 2. Various corrosion parameters for carbon steel in 1.0 M HCl in the absence and the presence of optimum concentration of Bip1 at different temperatures after 1h.

Temp (K)	Inhibitor	*A* (mg/cm^2 h)	η_w%	θ
	Blank	1.070	-----	-----
308	Bip1	0.020	98.1	0.981
	Blank	1.490	-----	-----
313	Bip1	0.049	96.7	0.967
	Blank	2.870	-----	-----
323	Bip1	0.215	92.5	0.925
	Blank	5.210	-----	-----
333	Bip1	0.724	86.1	0.861
	Blank	10.02	-----	-----
343	Bip1	2.465	75.4	0.754

Arrhenius plots for the corrosion rate of carbon steel were given in Fig. 4 and the result is shown in Table 3. Value of E_a for carbon steel in 1.0 M HCl with inhibitor and in the absence of inhibitor was estimated by calculating the slop of Ln (A) vs. 1/T. The linear regression coefficients are close to 1, indicating that the steel corrosion in hydrochloric acid can be elucidated using the kinetic model. The activation energy E_a values of the corrosion reaction in the absence and presence of Bip1 and Blank which are E_a = 55.75 kJ mol^{-1} for blank, E_a = 119.52 kJ mol^{-1} for Bip1, respectively**.** The increase in the apparent activation energy may be interpreted as physical adsorption that occurs in the first stage [46]. The increase in activation energy can be stated as to an appreciable decrease in the adsorption of the inhibitor on the carbon steel surface with increase in temperature. Desorption of inhibitor molecule occurs with decreases in adsorption as these two opposite processes are in equilibrium. As desorption increases of inhibitor molecules at higher temperatures, the greater surface area of carbon steel comes in contact with aggressive environment, resulting increased corrosion rates with increase in temperature [47].

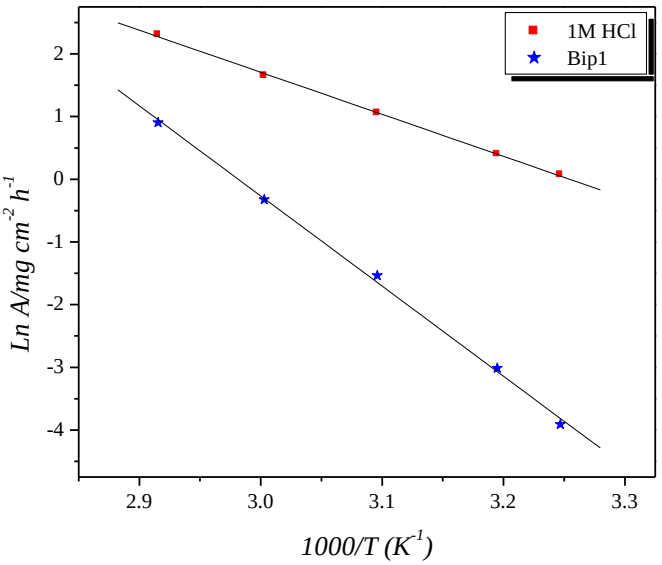

Figure 4. Arrhenius plots of Ln A vs. 1/T for steel in 1.0 M HCl in the absence and the presence of Bip1 at optimum concentration.

Table 3. Activation parameters for the steel dissolution in 1.0 M HCl in the absence and the presence of Bip1 at optimum concentration.

Inhibitor	A (mg/cm^2 h)	Linear regression coefficient (r)	E_a (kJ/mol)	ΔH_a (kJ/mol)	ΔS_a (J/mol K)
Blank	3.0066×10^{9}	0.99961	55.75	53.05	-72.49
Bip1	4.10874×10^{18}	0.99913	119.52	116.82	102.39

The enthalpy of activation, ΔH_a and entropy of activation ΔS_a were obtained from Eyring transition state equation:

$$A = \frac{RT}{Nh}\exp\left(\frac{\Delta S_a}{R}\right)\exp\left(-\frac{\Delta H_a}{RT}\right) \quad (6)$$

where A is the corrosion rate, h is the Planck's constant (6.626176 × 10^{-34} Js), N is the Avogadro's number (6.02252 × 1023 mol^{-1}), R is the universal gas constant and T is the absolute temperature. Fig. 5 shows a plot of Ln (A/T) against 1/T. Straight lines were obtained with a slope is equal to (ΔH_a /R) and intercept is equal to (Ln (R/Nh + ΔS_a /R))), from which the values of ΔH_a and ΔS_a were calculated and listed in Table 4. Bip1 is an organic nitrogen compound that easily protonates to give a cationic form in acid medium. The E_a value was greater than 20 kJ mol^{-1} in both the presence and absence of the inhibitor, which reveals that the entire process is controlled by the surface reaction [48].

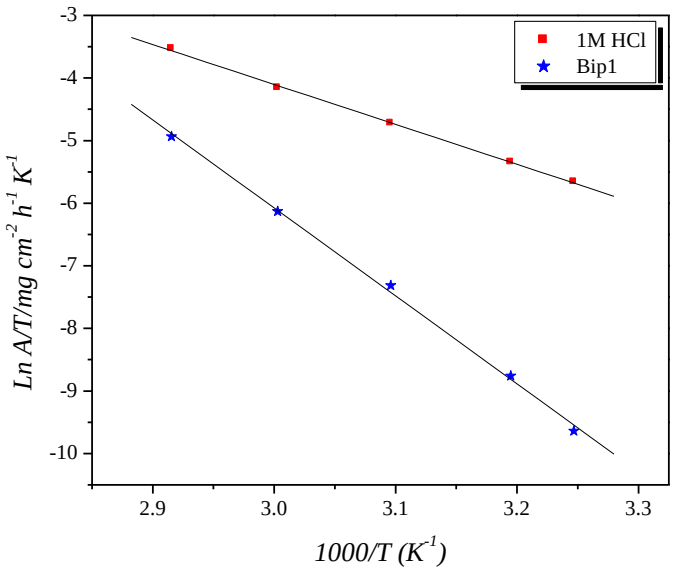

Figure 5. Arrhenius plots of Ln(A/T) vs. 1/T for steel in 1.0 M HCl in the absence and the presence of Bip1 at optimum concentration.

The values of ΔH_a and E_a are nearly the same and are higher in the presence of the inhibitor. This indicates that the energy barrier of the corrosion reaction increased in the presence of the inhibitor without changing the mechanism of dissolution. The positive values of ΔH_a for both corrosion processes with and without the inhibitor reveal the endothermic nature of the steel dissolution process and indicate that the dissolution of steel is difficult [49, 50].

The large negative value of ΔS_a for C38 steel in 1.0 M HCl implies that the activated complex is the rate-determining step, rather than the dissociation step. In the presence of the inhibitor, the value

of ΔS_a increases and is generally interpreted as an increase in disorder as the reactants are converted to the activated complexes [49]. The positive values of ΔS_a reflect the fact that the adsorption process is accompanied by an increase in entropy, which is the driving force for the adsorption of the inhibitor onto the steel surface.

3.1.3. Adsorption and thermodynamic considerations

Organic corrosion inhibitors are known to decrease metal dissolution via adsorption on the metal / corrodent interface to form a protective film which separates the metal surface from the corrosive medium. The adsorption route is usually regarded as a substitution process between the organic inhibitor in the aqueous solution [Inh $_{(sol)}$] and water molecules adsorbed at the metal surface [H_2O $_{(ads)}$] as follows [51, 52]:

$$Inh_{(sol)} + \chi H_2O_{(ads)} \leftrightarrow Inh_{(ads)} + \chi H_2O_{(sol)} \qquad (7)$$

where χ represents the number of water molecules replaced by one molecule of adsorbed inhibitor. The adsorption bond strength is dependent on the composition of the metal and corrodent, inhibitors components, concentration as well as temperature. In depth consideration of some of these variables will normally yield useful information regarding the adsorption mechanism. Although the complex nature of the corrosion inhibition process is not in doubt. Basic information on the interaction between the inhibitor and the metal surface can be provided by the adsorption isotherm.

The increase in efficiency of inhibition with increase in the Bip1 concentration indicates that the Bip1 is adsorbed on the steel surface at higher concentration leading to greater surface coverage. The surface coverage was evaluated from the expression: % η_w = θ ×100; assuming a direct relationship between inhibition efficiency (% η_w) and surface coverage (θ). Thus, in order to clarify the nature of adsorption, theoretical fitting of the surface coverage values to different isotherms were undertaken and the value of correlation coefficient (R^2) was used to determine the best fit isotherm. Langmuir adsorption isotherm was found to be the best fit. Langmuir isotherm is given by the expression [53]:

$$\frac{C_{\text{inh}}}{\theta} = \frac{1}{K_{\text{ads}}} + C_{\text{inh}} \qquad (8)$$

where K_{ads} is the adsorption constant, C_{inh} is the concentration of the inhibitor and surface coverage values (θ) are obtained from the weight loss measurements for various concentrations. Fig. 6 shows the C_{inh}/θ vs. C_{inh} for this inhibitor. The strong correlation (R^2 = 0.99999) demonstrates that adsorption of this inhibitor on carbon steel follow this isotherm and supposed that the adsorbed molecules occupy only one site and there are no interactions with other adsorbed species [54]. According to Eq. (8), K_{ads} can be calculated from intercept line on C_{inh}/θ axis. With the following equation, ΔG°_{ads} can be calculated from K_{ads}:

$$K_{ads} = (\frac{1}{55.5}) \exp(-\frac{\Delta G^{\circ}_{ads}}{RT}) \quad (9)$$

Where R is gas constant and T is absolute temperature of experiment and the constant value of 55.5 is the concentration of water in solution in mol dm^{-3}.

Table 4. Thermodynamic parameters for the adsorption of Bip1 in 1.0 M HCl on the carbon steel at 308K

Inhibitor	Slope	K_{ads} (M^{-1})	R^2	ΔG°_{ads} (kJ/mol)
Bip1	1.02	837436.77	0.99999	-45.21

The thermodynamic parameters for adsorption process obtained from Langmuir adsorption isotherm for the studied Bip1 molecule is given in Table 4. Results presented in the Table indicate that the value of ΔG°_{ads} is negative. The negative values also indicate a spontaneous adsorption of the inhibitor molecules.

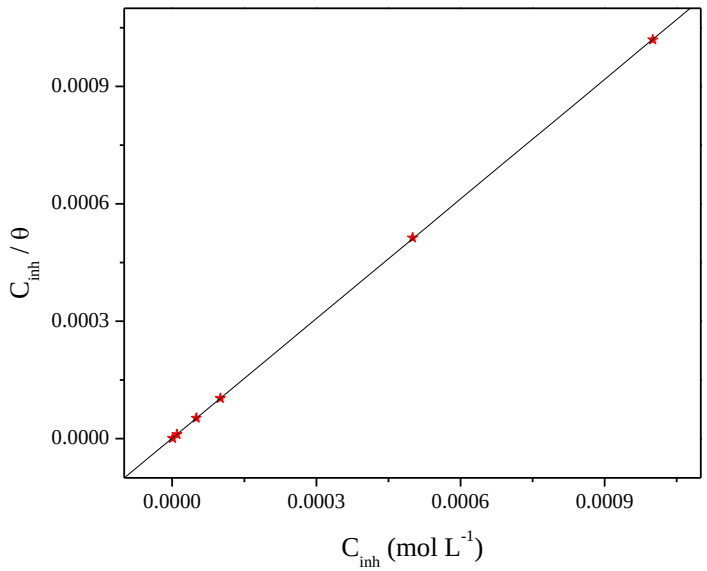

Figure 6. Langmuir adsorption of Bip1 on the carbon steel surface in 1.0 HCl solution.

Normally, the magnitude of ΔG°_{ads} around -20 kJ mol^{-1} or less negative is assumed for electrostatic interactions exist between inhibitor and the charged metal surface (i.e. physisorption). Those around -40 kJ mol^{-1} or more negative are indication of charge sharing or transferring from organic species to the metal surface to form a coordinate type of metal bond (i.e. chemisorption) [55]. Some authors have reported the values of ΔG°_{ads} less negative than -40 $kJmol^{-1}$for physical adsorption

frequently interpreted as the formation of an adsorptive film with an electrostatic character [54, 56]. The calculated ΔG°_{ads} value of slightly more negative than -40 kJ mol^{-1} indicate, therefore, that the adsorption mechanism of this bipyrazole derivative on steel in 1.0 M HCl solution was typical of chemisorption (Table 5).The unshared electron pairs in nitrogen may interact with d-orbital of steel to provide a protective chemisorbed film [57]. The heat of adsorption process (Q_{ads}) can also be estimated from the variation of surface coverage vs. reciprocal of temperature by using the Langmuir's adsorption isotherm as following [54, 58]:

$$Ln\left(\frac{\theta}{1-\theta}\right) = Ln(A) + Ln(C) - \frac{Q_{ads}}{RT} \qquad (10)$$

In this equation A is a constant and Q_{ads} is the heat of adsorption which is almost equal to enthalpy of adsorption process (ΔH°_{ads}). Fig.7. represents the variation of Ln (θ / (1 - θ)) versus 1/T at optimum concentration of inhibitor is. The heat of adsorption can be obtained from the slope of the line, which is equal to ($-Q_{ads}$ / R). The entropy of adsorption process (ΔS°_{ads}) can also be calculated based on the following thermodynamic basic equation [59, 60]:

$$\Delta G^{\circ}_{ads} = \Delta H^{\circ}_{ads} - T\Delta S^{\circ}_{ads} \qquad (11)$$

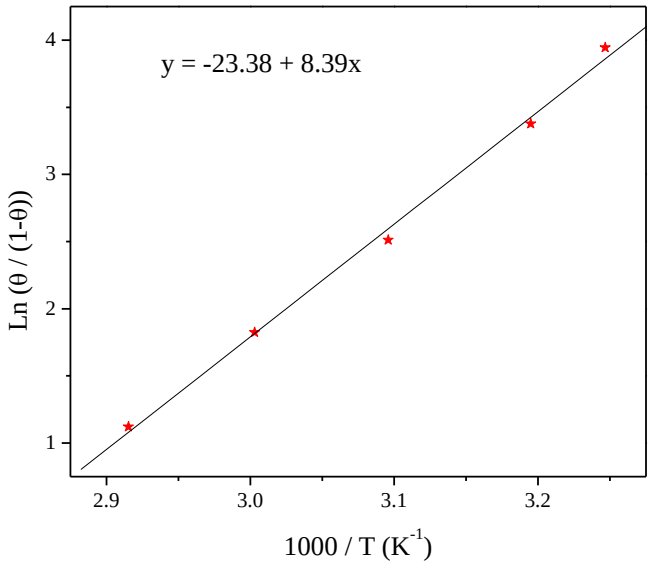

Figure 7. Ln (θ/1- θ) vs.1/T for adsorption of Bip1.

The heat of adsorption (Q_{ads}) and the entropy value of the inhibitor adsorption (ΔS°_{ads}) was calculated as described in the literature [61, 62] and found to be -69.75 kJmol^{-1} and -79.67 Jmol^{-1} K^{-1}, respectively. Since ΔH°_{ads} was negative, the adsorption of Bip1 molecules onto the carbon steel surface

was an exothermic process. In an exothermic process, physisorption can be distinguished from chemisorption by considering the absolute value of ΔH°_{ads}. For physisorption, ΔH°_{ads} is lower than 40 kJ mol^{-1}, while for chemisorption, ΔH°_{ads} approaches 100 kJ mol^{-1}. In the present study, the average ΔH°_{ads} value was almost equal to the common chemical adsorption heat, once again implying that chemical adsorption took place. ΔS°_{ads} is negative because inhibitor molecules freely moving in the balk solution, were adsorbed in an orderly fashion onto the carbon steel surface [63].

3.2. Tafel polarization study

Fig. 8 represents potentiodynamic polarization curves for carbon steel in 1.0 M HCl in the absence and presence of various concentration of this inhibitor. As can be seen both anodic and cathodic reactions of carbon steel with acid is inhibited in the presence of the inhibitor molecule. Thus, addition of this inhibitor molecule reduces the carbon steel dissolution as well as retarding the hydrogen evolution reaction. Table 6 shows the electrochemical corrosion parameters, as corrosion potential (E_{corr}), cathodic Tafel slopes (β_c), corrosion current density (I_{corr}), obtained by extrapolation of the Tafel lines and the inhibition efficiency ($\eta_{Tafel}(\%)$) which was evaluated from the relation:

$$\eta_{Tafel}(\%) = \frac{I_{corr} - I_{corr(i)}}{I_{corr}} \times 100 \qquad (12)$$

where I_{corr} and $I_{corr(i)}$ are the corrosion current densities for steel electrode in the uninhibited and inhibited solutions, respectively.

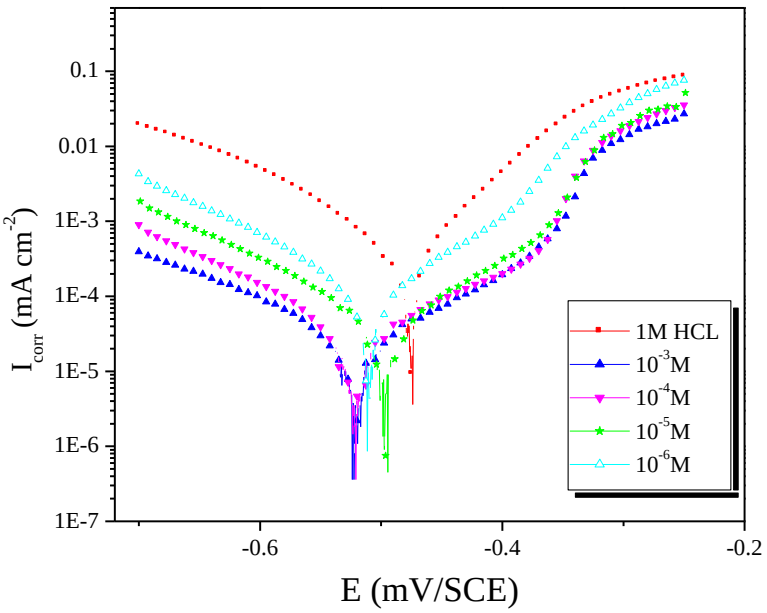

Figure 8. Polarisation curves of carbon steel in 1.0 M HCl for various concentrations of Bip1.

It is evident from Table 6 that the value of β_c slight changed, indicates that the cathodic corrosion mechanism of steel does not change. The corrosion current density (I_{corr}) decreased by the increase in the adsorption of the inhibitor with increasing inhibitor concentration. The values of η_{Tafel}(%) increase with the inhibitor concentration reaching its maximum value, 97.6% at 10^{-3}M. According to Ferreira et.al [64] and Li et. al. [65], if the displacement in corrosion potential is more than 85 mV with respect to the corrosion potential of the blank solution, the inhibitor can be consider as a cathodic or anodic type. In present study, maximum displacement was 46.7 mV with respect to the corrosion potential of the uninhibited sample which indicates that the studied inhibitor is a mixed type of inhibitor. The results obtained from the Tafel polarization showed good agreement with the results obtained from the weight loss measurements.

Table 6. Polarization data of C38 steel in 1.0 M HCl without and with addition of inhibitor at 308 K.

Inhibitor	Conc (M)	$-E_{corr}$ (mV/SCE)	$-\beta_c$ (mV dec^{-1})	I_{corr} (μA cm^{-2})	η_{Tafel} (%)
HCl	1	475.9	176	1077.8	-
Bip1	10^{-3}	521.8	161.6	25.7	97.6
	10^{-4}	522.6	151.0	43.5	96.0
	10^{-5}	498.5	160.8	59.0	93.3
	10^{-6}	510.9	155.9	142.1	86.8

3.3. Electrochemical impedance spectroscopy (EIS) studies

The corrosion behaviour of carbon steel in 1.0 M HCl in the absence and presence of Bip1 was investigated by EIS after immersion for 30 min at 308K. Nyquist plots of carbon steel in uninhibited and inhibited acid solutions containing various concentrations of Bip1 are presented in Fig. 10. EIS spectra obtained consists of one depressed semicircle. The increasing diameter of capacitive loop obtained in 1.0 M HCl in the presence of Bip1 indicated corrosion inhibition. The capacitive loop may be attributed to the charge transfer reaction. The increasing value of R_{ct} with increasing concentration indicated that the inhibitor molecules are adsorbed on the metallic surface and thereby inhibited the corrosion. The measured data were analyzed using the equivalent circuit given in figure 9. This circuit generally used to describe the iron/acid interface model [66]. This circuit gives an accurate fit to all experimental impedance data for Bip1. The equivalent circuit consists of solution resistance (R_s), charge transfer resistance (R_t) and a constant phase angle (CPE).

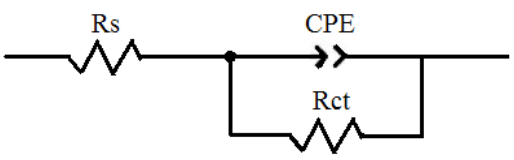

Figure 9. The electrochemical equivalent circuit used to fit the impedance measurements.

Corrosion kinetic parameters derived from EIS measurements and inhibition efficiencies are given in Table 7. It is apparent from Table 7 that the impedance of the inhibited system amplified with increasing inhibitor concentration and the C_{dl} values decreased with increasing inhibitor concentration. This decrease in C_{dl} results from a decrease in local dielectric constant and/or an increase in the thickness of the double layer, suggesting that inhibitor molecules inhibit the carbon steel corrosion by adsorption at the metal/acid interface [67].

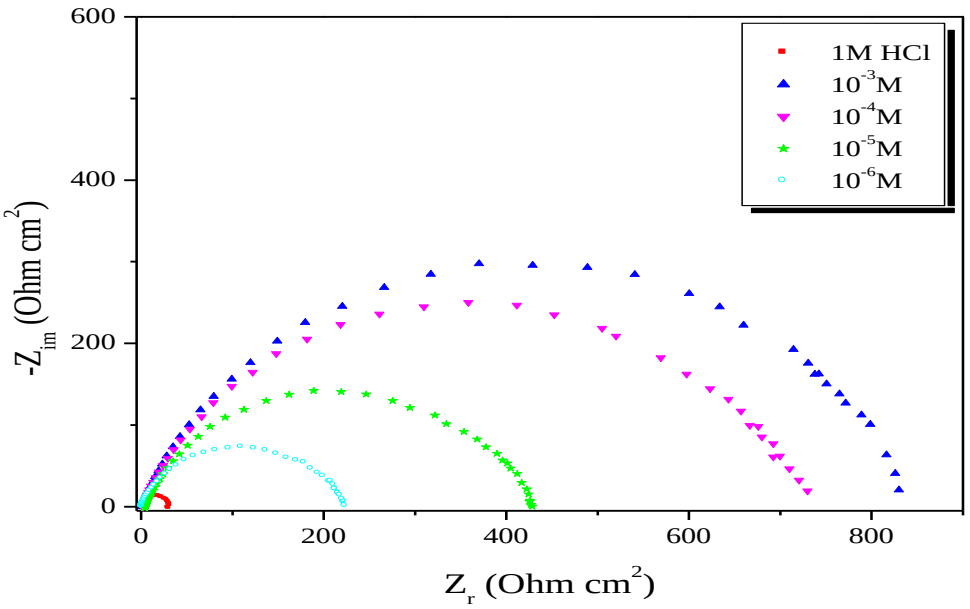

Figure 10. Nyquist diagrams for carbon steel in 1.0 M HCl containing different concentrations of Bip1 at 308 K.

The depression in Nyquist semicircles is a feature for solid electrodes and often referred to as frequency dispersion and attributed to the roughness and other inhomoge-nities of the solid electrode [68]. In this behaviour of solid electrodes, the parallel network: charge transfer resistance-double layer capacitance is established where an inhibitor is present. For the description of a frequency independent phase shift between an applied ac potential and its current response, a constant phase element (CPE) is used which is defined in impedance representa-tion as in Eq. (13) [69,70]:

$$Z_{CPE} = A^{-1} (i\,\omega)^{-n} \qquad (13)$$

where A is the CPE constant, ω is the angular frequency (in rad s^{-1}), i^2 =-1 is the imaginary number and n is a CPE exponent which can be used as a gauge of the heterogeneity or roughness of the surface [71]. Depending on the value of n, CPE can represent resistance (n= 0, A = R), capacitance (n=1, A = C), inductance (n = −1, A = L) or Warburg impedance (n = 0.5, A =W).

In this table are shown also the calculated "double layer capacitance" values, C_{dl}, derived from the CPE parameters according to [72]:

$$C_{dl} = (AR_{ct}^{1-n})^{1/n} \quad (14)$$

and the relaxation time constants according to the dielectric theory:

$$\tau = \frac{1}{2\pi f_{max}} \quad (15)$$

where f_{max} is the frequency at which appears the maximum in the curve -φ (phase shift) vs. log f. The inhibition efficiency η_z (%) is calculated by R_{ct} using Eq. (16), where R^0_{ct} and R_{ct} are the charge-transfer resistance values without and with inhibitor, respectively:

$$\eta_z(\%) = \frac{1/R_{ct}^{\circ} - 1/R_{ct}}{1/R_{ct}^{\circ}} \times 100 \quad (16)$$

Table 7. Impedance parameters for corrosion of steel in 1.0 M HCl in the absence and presence of different concentrations of Bip1 at 308 K.

Conc (M)	R_s (Ω cm^2)	R_{ct} (Ω cm^2)	n	A×10^{-4} (s^n Ω^{-1}cm^{-2})	C_{dl} (μF cm^{-2})	η_z (%)
Blank	1.67	29.66	0.91	0.14612	85.31	-----
10^{-3}	2.42	822.5	0.82	0.30583	13.63	96.4
10^{-4}	1.96	714.8	0.82	0.46267	21.89	95.8
10^{-5}	1.51	428.5	0.80	0.69273	28.75	93.3
10^{-6}	0.93	219.9	0.79	1.1618	43.82	86.5

4. MECHANISM OF INHIBITION

The transition of metal/solution interface from a state of active dissolution to the passive state is attributed to the adsorption of the inhibitor molecules and the metal surface, forming a protective film. The rate of adsorption is usually rapid and hence, the reactive metal surface is shielded from the aggressive environment [73]. Adsorption process can occur by electrostatic forces between ionic charges or dipoles of the adsorbed species and the electric charge on the metal surface can be expressed by its potential with respect to the zero charge potential (zcp) [74]. Also, the inhibitor molecules can be adsorbed to the metal surface via the electron transfer from the adsorbed species to the vacant electron orbital of low energy in the metal to form a coordinate type of link [75]. Adsorption of inhibitor molecules is often a displacement reaction involving removal of adsorbed water molecules from the metal surface. So that, during the adsorption of the inhibitor molecules on the metal surface, the change in the interaction energy with water molecules in passing from the dissolved to the adsorbed state form an important part of the free energy charge of adsorption process, ΔG°_{ads} .

The π-electron system of Bip1 possibly overlaps with the vacant d-orbital of the surface of iron resulting in a strong dπ–πp interaction. Surface coverage data (Table 1) shows that this additive is uniformly adsorbed over the metal surface but decreases with decrease in concentration of Bip1. Temperature influences the corrosion rate (Table 2) in the presence of Bip1. Corrosion rate, inhibition efficiency and surface coverage decrease with increase in temperature. At 10^{-3}M Bip1 inhibition efficiency reduces from 98.1% at 308K to 75.4% at 343K. The value of ΔG_{ads}° obtained indicates that Bip1 is strongly adsorbed on the carbon steel surface at all the temperatures studied but the adsorption decreases with increase in temperature.

5. CONCLUSION

2-[Bis-(3,5-dimethyl-pyrazol-1-ylmethyl)-amino]-pentanedioic acid (Bip1) was found to be an inhibitor for the corrosion of carbon steel in 1.0 M HCl solution. Inhibition efficiency increases with increase in Bip1 concentration, but decrease with increase in temperature. The adsorption Bip1 on carbon steel surface can be approximated by Langmuir isotherm model. The value of free energy of adsorption suggests strongly that Bip1 is adsorbed on carbon steel surface by chemical adsorption mechanism. Bip1 is a mixed-type inhibitor because both the cathodic and anodic curves decreased but corrosion potential remained constant. Impedance spectra show a high frequency capacitive loop related to the charge-transfer process of the metal corrosion and the double layer behaviour. The EIS spectra are described well by the proposed structural model of the interface carbon steel / 1.0 M HCl + Bip1.

ACKNOWLEDGEMENTS
Prof S. S. Al-Deyab and Prof B. Hammouti extend their appreciation to the Deanship of Scientific Research at king Saud University for funding the work through the research group project.

References

1. V.S. Sastri, Corrosion Inhibitors – Principles and Applications, Wiley, Chichester, England, 1998.
2. M. Lagrenee, B. Mernari, M. Bouanis, M. Traisnel, F. Bentiss, *Corros. Sci*. 44 (2002) 573.
3. M. Abdallah, *Corros. Sci*. 45 (2003) 2705.
4. H. Zarrok, S. S. Al-Deyab, A. Zarrouk, R. Salghi, B. Hammouti, H. Oudda, M. Bouachrine, F. Bentiss, *Int. J. Electrochem. Sc*i. 7 (2012) 4047.
5. H. Zarrok, H. Oudda, A. El Midaoui, A. Zarrouk, B. Hammouti, M. Ebn Touhami, A. Attayibat, S. Radi, R. Touzani, *Res. Chem. Intermed*. (2012) DOI: 10.1007/s11164-012-0525-x).
6. H. Zarrok, R. Salghi, A. Zarrouk, B. Hammouti, H. Oudda, Lh. Bazzi, L. Bammou, S. S. Al-Deyab. *Der Pharm. Chem*. 4 (2012) 407.
7. A.Ghazoui, R. Saddik, N. Benchat, B. Hammouti, M. Guenbour, A. Zarrouk, M. Ramdani, *Der Pharm. Chem.* 4 (2012) 352.
8. Zarrouk, B. Hammouti, H. Zarrok, R. Salghi, A. Dafali, Lh. Bazzi, L. Bammou, S. S. Al-Deyab, *Der Pharm. Chem*. 4 (2012) 337

9. H. Zarrok, S. S. Al-Deyab, A. Zarrouk, R. Salghi, B. Hammouti, H. Oudda, M. Bouachrine, F. Bentiss, *Int. J. Electrochem. Sci*. 7 (2012) 4047.
10. H. Zarrok, H. Oudda, A. El Midaoui, A. Zarrouk, B. Hammouti, M. Ebn Touhami, A. Attayibat, S. Radi, R. Touzani, *Res. Chem. Intermed*. (2012) DOI: 10.1007/s11164-012-0525-x).
11. H. Zarrok, R. Salghi, A. Zarrouk, B. Hammouti, H. Oudda, Lh. Bazzi, L. Bammou, S. S. Al-Deyab. *Der Pharm. Chem*. 4 (2012) 407.
12. A.Zarrouk, B. Hammouti, H. Zarrok, R. Salghi, A. Dafali, Lh. Bazzi, L. Bammou, S. S. Al-Deyab, *Der Pharm. Chem*. 4 (2012) 337.
13. Zarrouk, A. Dafali, B. Hammouti, H. Zarrok, S. Boukhris, M. Zertoubi, *Int. J. Electrochem. Sci*. 5 (2010) 46.
14. Zarrouk, T. Chelfi, A. Dafali, B. Hammouti, S.S. Al-Deyab, I. Warad, N. Benchat, M. Zertoubi, *Int. J. Electrochem. Sci*. 5 (2010) 696.
15. Zarrouk, I. Warad, B. Hammouti, A. Dafali, S.S. Al-Deyab, N. Benchat, *Int. J. Electrochem. Sci*. 5 (2010) 1516.
16. Zarrouk, B. Hammouti, R. Touzani, S.S. Al-Deyab, M. Zertoubi, A. Dafali, S. Elkadiri, *Int. J. Electrochem. Sci.* 6 (2011) 4939.
17. Zarrouk, B. Hammouti, H. Zarrok, S.S. Al-Deyab, M. Messali, *Int. J. Electrochem. Sci.* 6 (2011) 6261.
18. 18. A. Zarrouk, M. Messali, H. Zarrok, R. Salghi, A. Al-Sheikh Ali,B. Hammouti, S. S. Al-Deyab, F. Bentiss, *Int. J. Electrochem. Sci*., 7 (2012) 6998.
19. 19. A. Ghazoui, R. Saddik, N. Benchat, M. Guenbour, B. Hammouti, S.S. Al-Deyab, A. Zarrouk, *Int. J. Electrochem. Sci*., 7 (2012) 7080.
20. 20. A. Zarrouk, B. Hammouti, S.S. Al-Deyab, R. Salghi, H. Zarrok, C. Jama, F. Bentiss, *Int. J. Electrochem. Sci.*, 7 (2012) 5997.
21. I. B. Obot, N. O. Obi-Egbedi, *Corros. Sci*. 52 (2010) 198.
22. I. Ahamad, M. A. Quraishi, *Corros. Sci*. 51 (2009) 2006.
23. R. Touzani, A. Ramdani, T. Ben-Hadda, S. El Kadiri, O. Maury, H. Le Bozec, P.H. Dixneuf, *Synth. Commun*., 31 (2001) 1315.
24. A. El Ouafi, B. Hammouti, H. Oudda, S. Kertit, R. Touzani, A. Ramdani, *Anti-Corrosion Meth. Mater*. 49 (2002) 199.
25. A. Dafali, B. Hammouti, R. Touzani, S. Kertit, A. Ramdani, K. El Kacemi, *Anti-Corrosion Meth. Mater*. 49 (2002) 96.
26. R. Touzani, S. Garbacia, O. Lavastre, V.K. Yadav, B. Carboni, *J. Comb. Chem*. 5 (2003) 375.
27. S. Garbacia, C. Hillairet, R. Touzani, O. Lavastre, *Collec. Czech. Chem. Commun*/ 70 (2005) 34.
28. I. Bouabdallah, I. Zidane, B. Hacht, R. Touzani, A. Ramdani, *Arkivoc* 11 (2006) 1.
29. I. Bouabdallah, R. Touzani, I. Zidane, A. Ramdani, *Catal. Commun*. 8 (2007) 707.
30. I. Bouabdallah, R. Touzani, I. Zidane, A. Ramdani, *J. Iran. Chem. Soc.* 3 (2007) 299.
31. M. El Kodadi, F. Malek, R. Touzani, A. Ramdani, *Catal. Commun*. 9 (2008) 966.
32. N. Boussalah, R. Touzani, I. Bouabdallah, S. El Kadiri, S. Ghalem, *J. Mol. Catal. A Chem*. 306 (2009)113.
33. R. Touzani, A. Ramdani, S. El Kadiri, *Inter. J. Phys. Sci*. 4 (2009) 906.
34. A. Zerrouki, R. Touzani, S. El Kadiri. *Arab. J. Chem*. 4 (2011) 459.
35. Y. Toubi, R. Touzani, S. Radi, S. El Kadiri. *J. Environ. Mater. Sci*. 3 (2012) 328.
36. Ayse Ongun Yüce, Ramazan Solmaz, Gülfeza Kardas, *Mater. Chem. Phys*. 131 (2012) 615.
37. Dileep Kumar Yadav, M. A. Quraishi, B. Maiti, *Corros. Sci*. 55 (2012) 254.
38. I. B. Obot, N. O. Obi-Egbedi, *Curr. Appl. Phys*. 11 (2011) 382.
39. M. Benabdellah, R. Touzani, A. Aouniti, A. Dafali, S. El Kadiri, B. Hammouti, M. Benkaddour, *Mater. Chem. Phys*. 105 (2007) 373.
40. K. Tebbji, I. Bouabdellah, A. Aouniti, B. Hammouti, H. Oudda, M. Benkaddour, A. Ramdani, *Mater. Lett*. 61 (2007) 799.

41. N. Hackerman, E.S. Snavely, J.S. Payne, *J. Electrochem. Soc*. 113 (1966) 677.
42. T. Murakawa, S. Nagaura, N. Hackerman, *Corros. Sci*. 7 (1967) 79.
43. F.S.de Sauza, A.Spinelli, *Corros. Sci*. 51 (2009) 642.
44. A. Popova, E.Sokolova, M. Christov, *Corros. Sci*. 45 (2003) 33.
45. M.S. Morad, A.M. Kamal El-Dean, *Corros. Sci*. 48 (2006) 3398.
46. S. Martinez, I. Stern, *Appl. Surf. Sci*., 199 (2002) 83.
47. T. Szauer, A. Brand, *Electrochim. Acta*, 26 (1981) 1253.
48. L. Herrag, B. Hammouti, S. Elkadiri, A. Aouniti, C. Jama, H. Vezin, F. Bentiss, *Corros. Sci*. 52 (2010) 3042.
49. I. El Ouali, B. Hammouti, A. Aouniti, Y. Ramli, M. Azougagh, E. M. Essassi, M. Bouachrine, *J. Mater. Envir. Sci.* 1 (2010) 1.
50. 50. M. Behpour, S.M. Ghoreishi, N. Soltani, M. Salavati-Niasari, M. Hamadanian, A. Gandomi, *Corros. Sci*. 50 (2008) 2172.
51. E.E. Oguzie, Y. Li, F.H. Wang, *Electrochim. Acta*. 52 (2007) 6988.
52. M. Ameer, E. Khamis, G. Al-Senani, *J. Appl. Electrochem*., 32 (2002) 149.
53. U.F. Ekanem, S.A. Umoren, I.I. Udousoro, A.P. Udoh, *J. Mater. Sci*. 45 (2010) 5558.
54. G. Avci, *Colloid. Surf.* A. 317 (2008) 730.
55. S.A. Umoren, I.B. Obot, E.E. Ebenso, N.O. Obi-Egbedi, *Desalination.* 247 (2009) 561.
56. R. Solmaza, G. Kardas, M. Culh, B. Yazici, M. Erbil, *Electrochim. Acta*. 53 (2008) 5941.
57. F. Bentiss, M. Traisnel, M. Lagrene´e, *Corros.Sci*.42 (2000) 127.
58. S.M.A. Hosseini, A. Azimi, *Corros. Sci.* 51 (2009) 728.
59. A. Zarrouk, B. Hammouti, H. Zarrok, S. S. Al-Deyab, I. Warad, *Res. Chem. Intermed*., (2012) DOI 10.1007/s11164-012-0492-2.
60. B. Hammouti, A. Zarrouk, S.S. Al-Deyab And I. Warad, *Orient. J. Chem.*, 27 (2011) 23.
61. G. Mu, X. Li, G. Liu, *Corros. Sci*. 47 (2005) 1932.
62. H. Ashassi-Sorkhabi, B. Shaabani, D. Seifzadeh, *Appl. Surf. Sci*. 239 (2005) 154.
63. A. Y .Musa, A. A. H .Kadhum, A. B .Mohamad, A. Z. Daud, M. S. Takriff, S. K. Kamarudin, *Corros. Sci.* 51 (2009) 2393.
64. E.S. Ferreira, C. Giancomelli, F.C. Giacomelli, A. Spinelli, *Mater. Chem. Phys*. 83 (2004) 129.
65. W.H. Li, Q. He, C.L. Pei, B.R. Hou, *J. Appl. Electrochem*. 38 (2008) 289.
66. F. Mansfeld, *Corrosion.* 36 (1981)301.
67. H. Ashassi-Sorkhabi, D. Seifzadeh, MGEN. Hosseini, *Corros. Sci.*, 50 (2008) 3363.
68. A. Popova, M. Christova, *Corros. Sci*., 48 (2006) 3208.
69. Z. Stoynov, *Electrochim. Acta*. 35 (1990) 1493.
70. J.R. Macdonald, *J. Electroanal. Chem*. 223 (1987) 233.
71. J.W. Schultze, K. Wippermann, *Electrochim. Acta*. 32 (1987) 823.
72. S. Martinez, M. Metikoš-Hukovic´ , *J. Appl. Electrochem*. 33 (2003) 137.
73. C.Y. Chao, L.F. Lin, D.D. Macdonald, *J. Electrochem. Soc*. 128 (1981) 1187.
74. L.T. Intropor, In: Proceedings of the First International Congress on Metallic Corrosion, Butterworth, London, 1962, p. 147.
75. M.A. Migahed, I.F. Nassar, *Electrochem. Acta*. 53 (2008) 2877.